WILEY | Hindawi

Research Article

Astragaloside IV-PESV Repressed T Cell Immunosuppression by Inhibiting PD-L1 Expression in Prostate Cancer through STAT3 Pathway

Xujun You [iD],[1] Junfeng Qiu,[2] Qixin Li,[1] Qing Zhang,[1] Wen Sheng,[3] Wei Fu [iD],[1] and Yiguo Cao [iD][4]

[1]*Department of Andrology, Shenzhen Bao'an Traditional Chinese Medicine Hospital, Guangzhou University of Chinese Medicine, Shenzhen 518101, China*

[2]*Department of Andrology, Shenzhen Traditional Chinese Medicine Hospital, Guangzhou University of Chinese Medicine, Shenzhen 518033, China*

[3]*Andrology Laboratory, Hunan University of Chinese Medicine, Changsha 410208, China*

[4]*Department of Urology Surgery, Shenzhen Bao'an Traditional Chinese Medicine Hospital, Guangzhou University of Chinese Medicine, Shenzhen 518101, China*

Correspondence should be addressed to Wei Fu; fuwei84@gzucm.edu.cn and Yiguo Cao; caoyiguo82@gzucm.edu.cn

Background. Prostate cancer (PCa) is a major threat to men's health worldwide, and there is an urgent need to find a supportive strategy to improve traditional PD-1/PD-L1 targeted immunotherapy. Our previous research identified astragaloside IV and polypeptide extract from scorpion venom (PESV) as the main active components of the astragalus-scorpion drug pair for treating PCa. In this study, we wanted to continue exploring the modulatory effect of astragaloside IV-PESV on the immune microenvironment of tumors further to investigate the antitumor efficacy mechanism of astragaloside IV-PESV. *Methods.* First, molecular docking was performed to verify whether astragaloside IV and PESV could bind to STAT3 and PD-L1. Next, we performed mouse tumorigenesis experiments to explore the role of astragaloside IV-PESV. Additionally, we further validated the effects of astragaloside IV-PESV on the STAT3/PD-L1 pathway and immunity by *in vitro* cellular experiments. Furthermore, we overexpressed STAT3 and validated the effects of overexpression of STAT3 on cellular function, T cell activation, and immune escape *in vitro* and *in vivo*. *Results.* Molecular docking revealed astragaloside IV and PESV bound to STAT3 and PD-L1. Astragaloside IV-PESV led to notable tumor tissue volume and weight repression and inhibited tumor immunity and STAT3/PD-L1 pathway-related protein expressions. *In vitro*, astragaloside IV-PESV suppressed PD-L1 expression by inhibiting STAT3 signaling to modulate immunity. In contrast, overexpression of STAT3 restored PCa cell proliferation, migration, and invasion inhibition by astragaloside IV-PESV. In addition, overexpression of STAT3 restored the promoting effect of astragaloside IV-PESV on T cell activation. Finally, *in vivo* experiments further illuminated that overexpression of STAT3 restored the immune escape effect of astragaloside IV-PESV on the tumor. *Conclusion.* Astragaloside IV-PESV improved T cell immune escape by inhibiting PD-L1 expression in PCa through the STAT3 pathway.

1. Introduction

Prostate cancer (PCa) has a high morbidity and mortality rate and is a major threat to men's health worldwide. The morbidity and mortality of PCa continue to increase yearly due to its early symptoms that are not easily detected and limited screening conditions [1]. From a clinical, morphological, and molecular perspective, PCa is a heterogeneous disease [2]. Current treatment options include androgen receptor- (AR-) targeted drugs, chemotherapy, radionuclides, and the poly (ADP-ribose) inhibitor olaparib [3]. Although androgen deprivation therapy is effective in

advanced PCa, it still does not prevent the development of metastatic desmoplastic-resistant PCa [4]. The behaviors of cell proliferation, migration, invasion, and epithelial-mesenchymal transition (EMT) are the main drivers of malignant growth, metastatic spread, and resistance to treatment in PCa [5, 6]. Furthermore, these behaviors of tumor cells can be linked to immune cells in the tumor microenvironment, further promoting tumor development by inhibiting immune cell function [7, 8]. Therefore, it is crucial to investigate novel immunotherapies to treat PCa.

The interaction between the programmed cell death protein-1 (PD-1) and its ligand (PD-L1) is essential to suppress activated T lymphocytes [9]. By regulating PD-L1, tumor cells promote tumor proliferation, invasion, angiogenesis, and EMT on the one hand and suppress CD8$^+$ cytotoxic T cells mediating the immune escape process of tumor cells on the other hand [10–13]. Therefore, targeting the PD-1/PD-L1 axis is a potential anticancer strategy whose clinical value has been demonstrated in various cancers, including non-small-cell lung cancer (NSCLC) [14], gastric cancer [15], and liver cancer [16]. Studies have shown that STAT3 could act directly on PD-L1 promoter to induce PD-L1 expression in tumor cells and is involved in regulating PCa development [17, 18]. However, many patients, especially PCa, are ineffective against PD-1/PD-L1 therapy, and therefore, there is an urgent need to seek a supportive strategy to improve conventional PD-1/PD-L1-targeted immunotherapy [19].

Our previous research found that astragaloside IV and polypeptide extract from scorpion venom (PESV) were the main active components of the astragalus-scorpion drug pair for treating PCa [20]. He et al. reported that astragaloside IV enhanced PCa carboplatin sensitivity by inhibiting the AKT/NF-κB signaling pathway [21]. Zhang et al. revealed that PESV induced growth inhibition and apoptosis of PCa cells DU145 or could be used to treat PCa [22]. Due to the wide range of pharmacological effects of traditional Chinese medicine (TCM), we continued to investigate the modulating effect of astragaloside IV-PESV on tumor immune microenvironment on this basis further to investigate the antitumor pharmacological mechanism of astragaloside IV-PESV and provide sufficient clinical antitumor application of astragaloside IV-PESV.

2. Materials and Methods

2.1. Animals. C57BL/6 male mice (six-week-old) were ordered from Hunan SJA Laboratory Animal Co. Ltd. After one week of acclimatization, RM-1 (a mouse PCa cell line derived from C57BL/6 mice) was inoculated subcutaneously (1×10^6 cells per mouse in an injection volume of 100μL) into right axilla of mice to establish a homologous tumor mouse model [23]. After tumor implantation, the tumors were measured and observed every three days. After the formation of tumors (6 d after implantation), mice were grouped and treated with astragaloside IV, PESV, or astragaloside IV-PESV mixture. The groups were Control, astragaloside IV, PESV, and astragaloside IV-PESV, with 6 mice in each group. Astragaloside IV was administered at 40 mg/kg dose by

gavage [24], and PESV was administered at a dose of 1.2 mg/kg by intraperitoneal injection, both with saline as solvent. The source and dosage of astragaloside IV and PESV are consistent with our previous study [20]. The control group was given the same volume of saline by gavage or intraperitoneal injection. In addition, ov-NC or ov-STAT3-treated RM-1 was subcutaneously inoculated (1×10^6 cells per mouse) into the right axilla of mice. After the formation of tumors (6 d after implantation), mice were grouped and treated with astragaloside IV-PESV mixture. The groups were ov-NC, ov-STAT3, astragaloside IV-PESV + ov-NC, and astragaloside IV-PESV + ov-STAT3, with 6 mice in each group. The ov-NC and ov-STAT3 groups were given the same volume of saline by gavage or injection. Kinetics of tumor growth were analyzed every 3 days by caliper measurements. The tumor volume was measured by using a vernier caliper to measure the longest axis (L) and shortest axis (W) in the tumor body (the position of the longest axis and shortest axis was determined visually) and then using a simplified formula: tumor volume = $(W \times W \times L)/2$. According to the tumor growth, the experiment was ended after 21 d of tumor seeding, and the tumor tissues were removed and weighed. All animal experiments were approved by the Experimental Animal Ethics Committee of Guangzhou University of Chinese Medicine (No. 20210224026).

2.2. Cell Culture and Treatment. PC3 (human PCa cell, AW-CCH111) and RM-1 (AW-CCM416) were purchased from Abiowell. PC3 and RM-1 were cultured in F12K or Dulbecco's modified eagle medium (DMEM) with 10% fetal bovine serum (FBS) and 1% penicillin/streptomycin at 37°C and 5% CO$_2$, respectively. According to a previous study, 10μM astragaloside IV and 40 mg/mL PESV were given [20]. The experimental groupings were Control, astragaloside IV, PESV, and astragaloside IV-PESV. RM-1 and PC3 cells at logarithmic growth stage were plated in 6-well plates and treated with the following groupings: Control + T cells (PCa cells co-cultured with T cells), astragaloside IV + T cells (astragaloside IV-treated PCa cells and co-cultured with T cells), PESV + T cells (PESV-treated PCa cells and co-cultured with T cells), and astragaloside IV-PESV + T cells (astragaloside IV-PESV-treated PCa cells and co-cultured with T cells). In addition, STAT3 was overexpressed and divided into the ov-NC and ov-STAT3 groups. It was further grouped into Control, astragaloside IV-PESV, astragaloside IV-PESV + ov-NC, and astragaloside IV-PESV + ov-STAT3. Additionally, we performed a co-culture combined with astragaloside IV-PESV and ov-STAT3 treatment, and they were divided into Control + T cells (PCa cells co-cultured with T cells), astragaloside IV-PESV + T cells (astragaloside IV-treated PCa cells and co-cultured with T cells), astragaloside IV-PESV + ov-NC + T cells (astragaloside IV-PESV treated ov-NC transfected PCa cells and co-cultured with T cells), and astragaloside IV-PESV + ov-STAT3 + T cells (astragaloside IV-PESV treated ov-STAT3 transfected PCa cells and co-cultured with T cells). Lipofectamine 2000 (11668-019, Invitrogen) was used to transfect ov-NC and ov-STAT3. Plasmids ov-NC and ov-STAT3 were purchased from HonorGene.

2.3. Quantitative Real-Time PCR (qRT-PCR). Total cellular RNA was extracted using Trizol. To reverse transcribe RNA into cDNA, a cDNA reverse transcription kit (#CW2569, CWBIO) was used, and relative expression of genes was examined on a fluorescent quantitative PCR instrument (QuantStudio 1, Thermofisher) system by applying Ultra SYBR Mixture (#CW2601, CWBIO). Gene levels were calculated by the $2^{-\Delta\Delta Ct}$ method with β-actin as the internal reference gene. Primer sequences are STAT3-F: CAATAC CATTGACCTGCCGAT, STAT3-R: GAGCGACTCAAA CTGCCCT; PD-L1-F: AAAGACGAGCATAGCCGAAC, PD-L1-R: GCCACACCAATCCAACACC; β-actin-F: ACA TCCGTAAAGACCTCTATGCC, β-actin-R: TACTCCTGC TTGCTGATCCAC.

2.4. Western Blot. Total proteins were isolated by RIPA (AWB0136, Abiowell) and quantified using the BCA kit (AWB0104, Abiowell). Total proteins underwent 10% SDS-PAGE separation and were transferred to the NC membranes. After blocking, membranes were thoroughly mixed overnight with STAT3 (1 : 2000, 10253-2-AP, Proteintech), p-STAT3 (1 : 5000, ab76315, Abcam), PD-L1 (1 : 600, 28076-1-AP, Proteintech), and β-actin (1 : 5000, 66009-1-Ig, Proteintech). Subsequently, membranes were incubated with HRP-labeled secondary antibodies. ECL Plus luminescent solution (AWB0005, Abiowell) was co-incubated with the membranes, and then a gel imaging system (ChemiScope6100, CLINX) was used to visualize and analyze the protein bands.

2.5. Immunohistochemistry (IHC). Tumor tissue sections were subjected to antigenic thermal repair using EDTA buffer (pH 9.0) and boiling water. Appropriate dilutions of anti-Ki67 (1 : 500, ab1666, Abcam) and CD8 (1 : 200, AWA55833, Abiowell) were added dropwise overnight at 4°C. PBS was rinsed for 5 min, 3 times. 50–100 μL Anti-Rabbit IgG (PV-9001, ZSGB-BIO) antibody was incubated at 37°C. DAB was performed for color development, and then, sections were observed using a fluorescence microscope (BA210T, Motic).

2.6. Immunofluorescence (IF). PC3 cells and RM-1 cells were fixed with 4% paraformaldehyde. 0.3% tretinoin was added and permeabilized at 37°C. Cells were blocked at 37°C with 5% bovine serum albumin (BSA) for 1 h. Primary antibodies p-STAT3 (1 : 50, AF3293, Affinity) and PD-L1 (1 : 50, ab213524, Abcam) were added overnight. Then 50–100 μL Goat Anti-Rabbit IgG (H + L) secondary antibody Alexa Fluor 488 (1 : 200, AWS0005b, Abiowell) was added and incubated at 37°C. Nuclei were stained with DAPI. Slices were blocked in buffered glycerol and observed by fluorescence microscopy (BA210T, Motic).

2.7. Flow Cytometry. CD3+ CD8+ T cell levels in tumor tissues and peripheral blood were first detected by flow cytometry. The tumor was ground on a 70 μm filter to obtain a cell suspension. 1500 rpm centrifugation was performed to remove the supernatant, and 5 mL erythrocyte lysis was added to lyse cells and then centrifuged. The supernatant was removed, and the cells were re-suspended with a basal medium. For blood, 5 mL PBS was added to fresh blood and mixed with the liquid surface of 10 mL cell separation solution. Cells were centrifuged at 400 g (approximately 1500 rpm, 15 cm radius horizontal rotor) for 20 min. Then, we collected the second layer of cells and added 6 mL of PBS buffer into the centrifuge tube, mixed thoroughly, and then centrifuged cells at 400 g (about 1500 rpm) for 20 min. 5 mL of erythrocyte lysis solution was added, and then cells were lysed for 3 min and centrifuged. 7 mL of PBS was added to resuspend cell precipitate and centrifuged. After the residue was washed twice, then lymphocytes were obtained. Subsequently, the abovetreated cells were centrifuged, the supernatant was discarded, the cell precipitate was resuspended with 100 μL of basal medium, and the corresponding CD3 (17-0031-82, eBioscience) and CD8 (17-0081-82, eBioscience) antibodies were added, mixed well, and incubated for 30 min and protected from light. At the same time, the non-stained and single-stained tubes were set up. Cells were washed with 1 mL of 0.5% BSA-PBS and centrifuged. Then, the supernatant was discarded, and 150 μL of 0.5% BSA-PBS was used to resuspend cells for flow cytometry detection.

In addition, T cell apoptosis was detected by flow cytometry. Cells were collected by digestion with EDTA-free trypsin, and cells were centrifuged at 2000 rpm for 5 min each time to collect about 3.2×10^5 cells. 500 μL binding buffer, 5 μL APC, and 5 μL propidium iodide were added and mixed well. The reaction was performed away from light. Within 1 h, cells were observed and detected using flow cytometry.

2.8. Cell Counting Kit 8 (CCK-8) Assay. Cells were counted using a digestion method and then inoculated into 96-well plates at a density of 5×10^3 cells/well/100 μL. Subsequently, each well was supplemented with 10 μL of CCK-8 solution (NU679, Dojindo). After incubating the plates at 37°C for 4 h, the absorbance values at 450 nm were examined and recorded.

2.9. Transwell Assays. The migration ability of cells was determined through transwell chambers (3428, Corning). 1×10^6/mL of cells was resuspended in serum-free medium, and 100 μL of cell suspension was added to transwell chambers' upper chamber. The lower chamber was incubated with a complete medium with 10% FBS for 48 h. The culture medium in the chambers was discarded. Cells on the upper chamber were wiped off with a wet cotton swab, fixed with 4% paraformaldehyde, and stained with 0.5% crystal violet (AWC0333, Abiowell) for 5 min. Photos of cells on the upper chamber's outer surface were taken under an Olympus microscope (Japan). Cell invasion assays were performed with transwell chambers with matrix gel (#356231, Corning) [25].

2.10. Enzyme-Linked Immunosorbent Assay (ELISA). IFN-γ (mouse-KE10001, human-KE00146, Proteintech), TNF-α (mouse-KE10002, human-KE00154, Proteintech), Granzyme-B (GZMB, mouse-CSB-E08720m, human-CSB-E08718h, CUSABIO), and Perforin (mouse-CSB-E13429m, human-CSB-E09313h, CUSABIO) kits were used to evaluate IFN-γ, TNF-α, GZMB, and Perforin levels in peripheral blood and cell supernatants.

2.11. Bioinformatics Prediction and Chromatin Immunoprecipitation (ChIP). The potential binding site of STAT3 in the promoter region of PD-L1 (ch9: 5449027–5449342) was first predicted by the UCSC ChIP database (https://genome.ucsc.edu/index.html). Next, the potential binding of STAT3 to the PD-L1 promoter region was further verified by ChIP experiments [26]. Cells were cross-linked with 1.1% formaldehyde chromatin and sonicated for fragmentation. DNA fragment length was then examined, and DNA was immunoprecipitated with antibodies specific to the target protein against STAT3. Immunoprecipitation products were collected after incubation with G protein agarose beads. Subsequently, uncrosslinking and DNA purification were performed. After DNA purification, PD-L1 promoter binding sites were assessed by qRT-PCR. Primer sequences are PD-L1-F: ATGCTCCTGCCAAATCAA, PD-L1-R: CGT TGTTTGCCTTTCCTT.

2.12. Docking Research. Docking studies of astragaloside IV and PESV with STAT3 and PD-L1 proteins were performed with AutoDock Vina 1.1.2 software. PyMOL and LigPlot were then applied for visualization and analysis.

2.13. Statistical Analysis. Measurement data were analyzed using GraphPad Prism8.0 software with mean ± standard deviation as the measure of statistical significance. Comparing groups was done using Student's *t*-test, and multigroup comparisons were done using one-way analysis of variance (ANOVA). A statistically significant difference was indicated by $P < 0.05$.

3. Results

3.1. Molecular Docking Validated Astragaloside IV and PESV Bound to STAT3 and PD-L1. First, we verified whether astragaloside IV and PESV could bind to STAT3 and PD-L1 by molecular docking. The results of molecular docking of astragaloside IV with STAT3 and PD-L1 are shown in Figure 1(a). Astragaloside IV could bind to STAT3 and PD-L1 protein and interact with the surrounding amino acids. The docking binding energy was −8.3 kcal/mol (STAT3) and −9.5 kcal/mol (PD-L1), respectively, indicating that astragaloside IV could bind spontaneously to STAT3 and PD-L1 proteins. PESV (LPDKVPIR peptide) was able to spontaneously bind to STAT3 and PD-L1 proteins (Figure 1(b)). The docking binding energies were −5.9 kcal/mol (STAT3) and −5.2 kcal/mol (PD-L1), respectively. In addition, PESV (VRDGYIADDK peptide) could

spontaneously bind to STAT3 and PD-L1 proteins (Figure 1(c)). The docking binding energies were −6.4 kcal/mol (STAT3) and −6.8 kcal/mol (PD-L1), respectively (Table 1). These results indicated that astragaloside IV and PESV could bind to STAT3 and PD-L1.

3.2. Astragaloside IV-PESV Repressed Immunosuppression and STAT3/PD-L1 Pathway. Next, we performed tumorigenic experiments in mice to explore the role of astragaloside IV-PESV. Compared with the Control group, astragaloside IV, PESV, and astragaloside IV-PESV groups showed a significant reduction in tumor volume and weight and decreased Ki-67 expression (Figures 2(a)–2(c)). CD8 levels were increased in astragaloside IV, PESV, and astragaloside IV-PESV groups than in the Control group (Figure 2(d)). Furthermore, astragaloside IV, PESV, and astragaloside IV-PESV treatment notably increased CD3+ CD8+ T cell levels in tumor tissues and peripheral blood, with the most obvious increase after astragaloside IV-PESV treatment (Figure 2(e)). In addition, IFN-γ, TNF-α, GZMB, and Perforin levels in peripheral blood were also increased after astragaloside IV, PESV, and astragaloside IV-PESV treatment (Figure 2(f)). p-STAT3 and PD-L1 levels were decreased in astragaloside IV, PESV, and astragaloside IV-PESV groups than in the Control group. STAT3 expression did not change significantly (Figure 2(g)). Taken together, astragaloside IV-PESV repressed immunosuppression and STAT3/PD-L1 pathway.

3.3. Astragaloside IV-PESV Suppressed PD-L1 Expression by Inhibiting STAT3 Signaling to Regulate Immunity. Next, we further validated astragaloside IV-PESV effects on STAT3/PD-L1 pathway and immunity by *in vitro* cellular assays. Compared with the Control group, p-STAT3 and PD-L1 levels were significantly reduced in the astragaloside IV, PESV, and astragaloside IV-PESV groups of PC3 and RM-1 cells. STAT3 expression did not change significantly (Figures 3(a), 3(b), and S1A). After co-culture with T cells, we found that astragaloside IV, PESV, and astragaloside IV-PESV treatment decreased T cell apoptosis and increased cell supernatant IFN-γ, TNF-α, GZMB, and Perforin levels (Figures 3(c) and 3(d)). Among them, astragaloside IV-PESV treatment had the most obvious effect. In addition, we constructed overexpression STAT3 plasmids. STAT3 level was signally elevated in the ov-STAT3 group than in the ov-NC group, indicating that we successfully transfected the overexpression STAT3 plasmids (Figures 3(e) and S1B). Furthermore, we found that astragaloside IV-PESV + ov-STAT3 significantly reversed the decrease in STAT3, p-STAT3, and PD-L1 expression compared to the astragaloside IV-PESV + ov-NC group (Figures 3(f) and S1C). Moreover, our ChIP experiments further demonstrated that astragaloside IV-PESV could inhibit the binding of STAT3 to the PD-L1 promoter (Figure 3(g)). These results revealed that astragaloside IV-PESV suppressed PD-L1 expression by inhibiting STAT3 signaling to regulate immunity.

astragaloside IV-PD-L1

astragaloside IV-STAT3

(a)

PESV (LPDKVPIR)-PD-L1

PESV (LPDKVPIR)-STAT3

(b)

PESV (VRDGYIADDK)-PD-L1
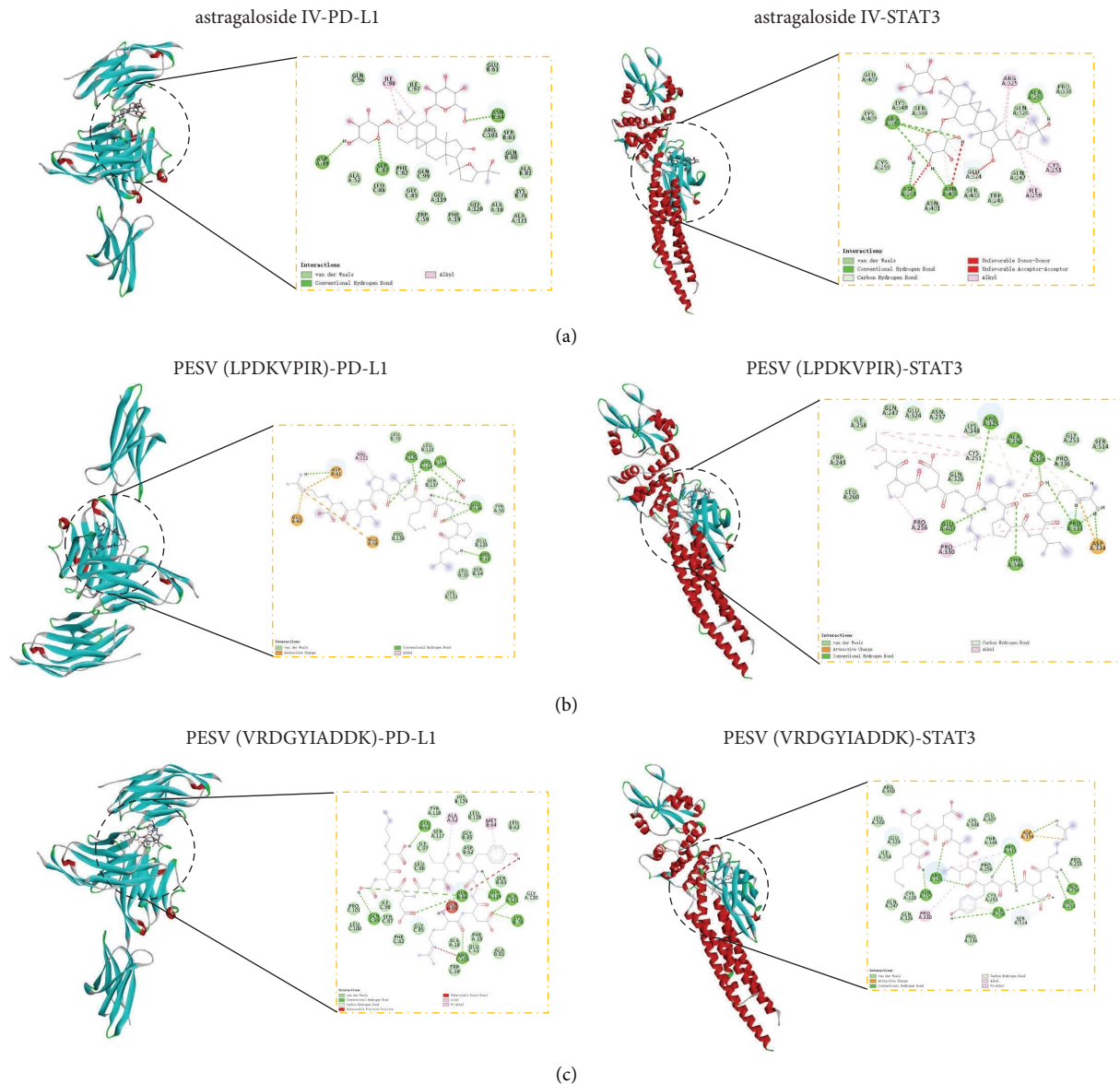
PESV (VRDGYIADDK)-STAT3

(c)

FIGURE 1: Molecular docking validated astragaloside IV and PESV bound to STAT3 and PD-L1. (a) Molecular docking of the interaction of astragaloside IV with STAT3 and PD-L1. (b) Molecular docking of the interaction of PESV (LPDKVPIR peptide) with STAT3 and PD-L1. (c) Molecular docking of the interaction of PESV (VRDGYIADDK peptide) with STAT3 and PD-L1.

TABLE 1: The results of docking research.

Ligand	Protein	Binding energies (kcal/mol)
Astragaloside IV	STAT3	−8.3
	PD-L1	−9.5
PESV (LPDKVPIR peptide fragment)	STAT3	−5.9
	PD-L1	−5.2
PESV (VRDGYIADDK peptide fragment)	STAT3	−6.4
	PD-L1	−6.8

3.4. Overexpression of STAT3 Reversed the Inhibitory Effects of Astragaloside IV-PESV on PCa Cell Function. Next, we examined the effect of overexpression of STAT3 on cell function. Compared with the Control group, proliferation, migration, and invasion ability of PCa cells were decreased in the astragaloside IV-PESV group. In contrast, proliferation, migration, and invasion ability of PCa cells were enhanced after overexpression of STAT3 (Figures 4(a)–4(c)). These
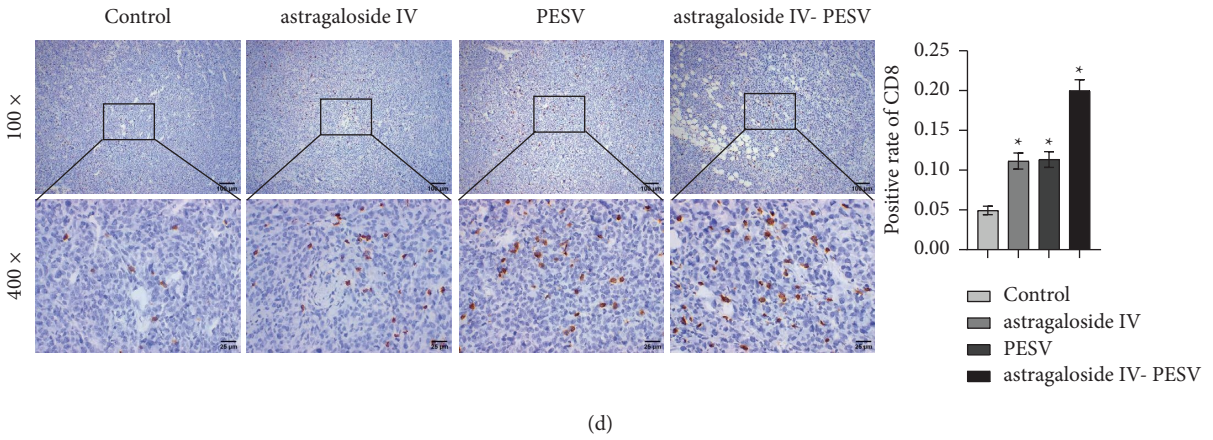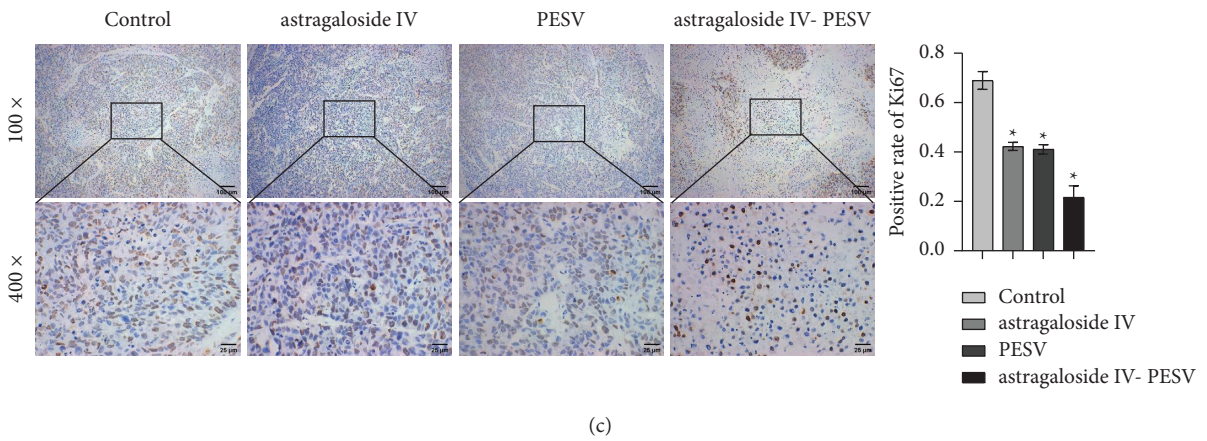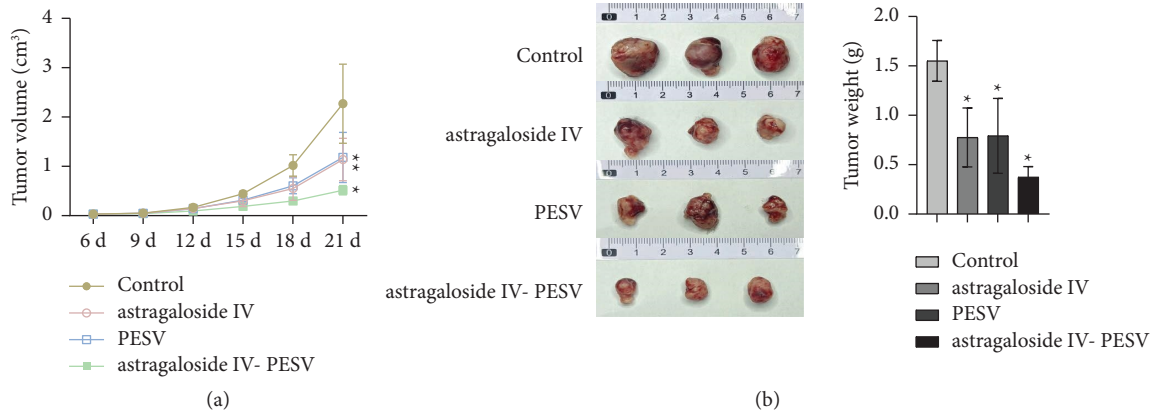
(a)
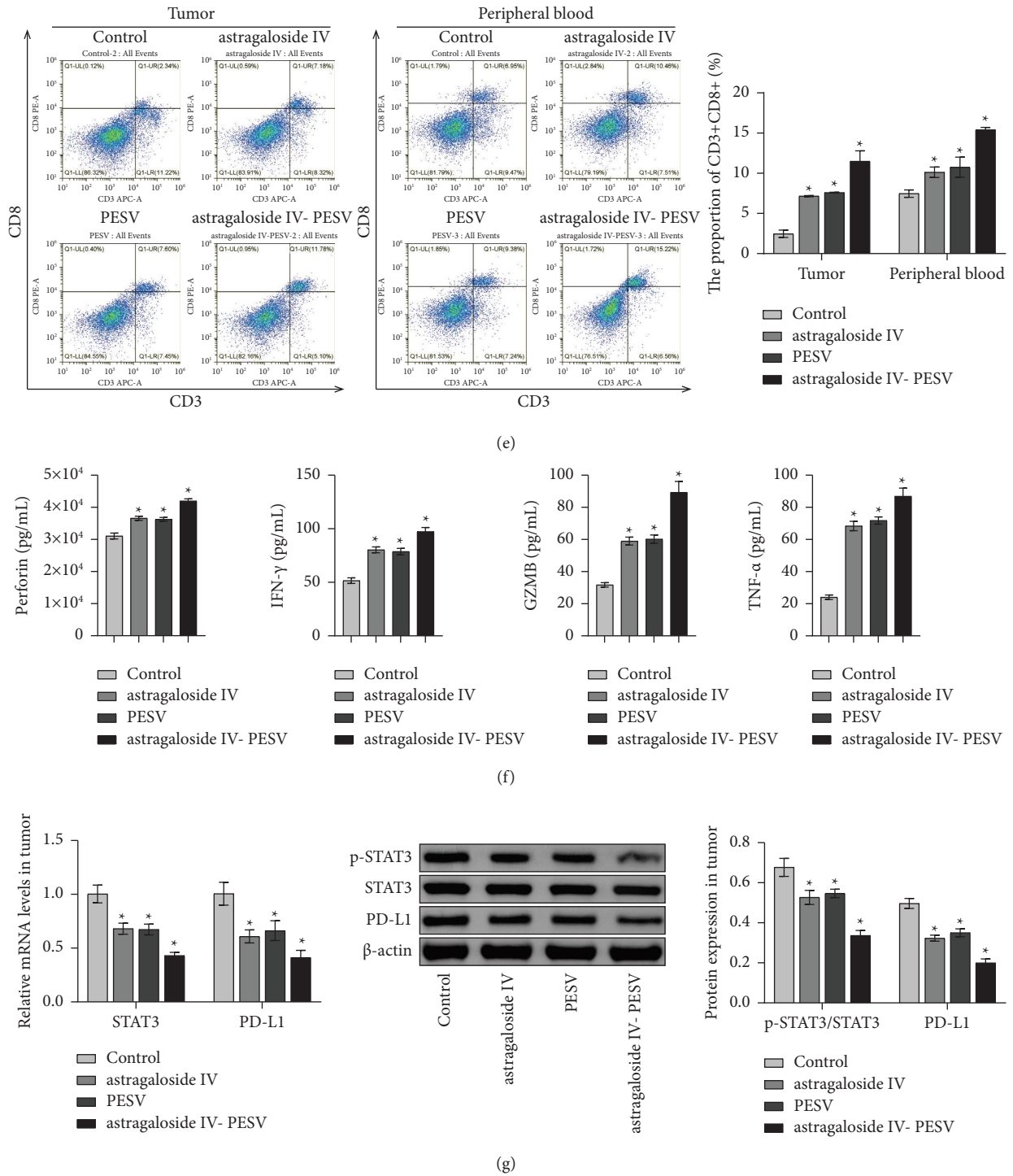
(b)

(c)

(d)

Figure 2: Continued.

(e)

(f)

(g)

FIGURE 2: Astragaloside IV-PESV repressed immunosuppression and STAT3/PD-L1 pathway. (a) Tumor volume. (b) The image of tumor tissues and the weight of tumor tissues. (c) IHC analysis for Ki-67 expression. (d) IHC analysis for CD8 expression. (e) Flow cytometry of CD3+ CD8+ T cells in tumor tissues and peripheral blood. (f) ELISA of IFN-γ, TNF-α, GZMB, and Perforin levels in peripheral blood. (g) p-STAT3, STAT3, and PD-L1 levels in tumor tissues. $^*P < 0.05$ vs. Control.

(a)

(b)

(c)

(d)

(e)   (f)   (g)
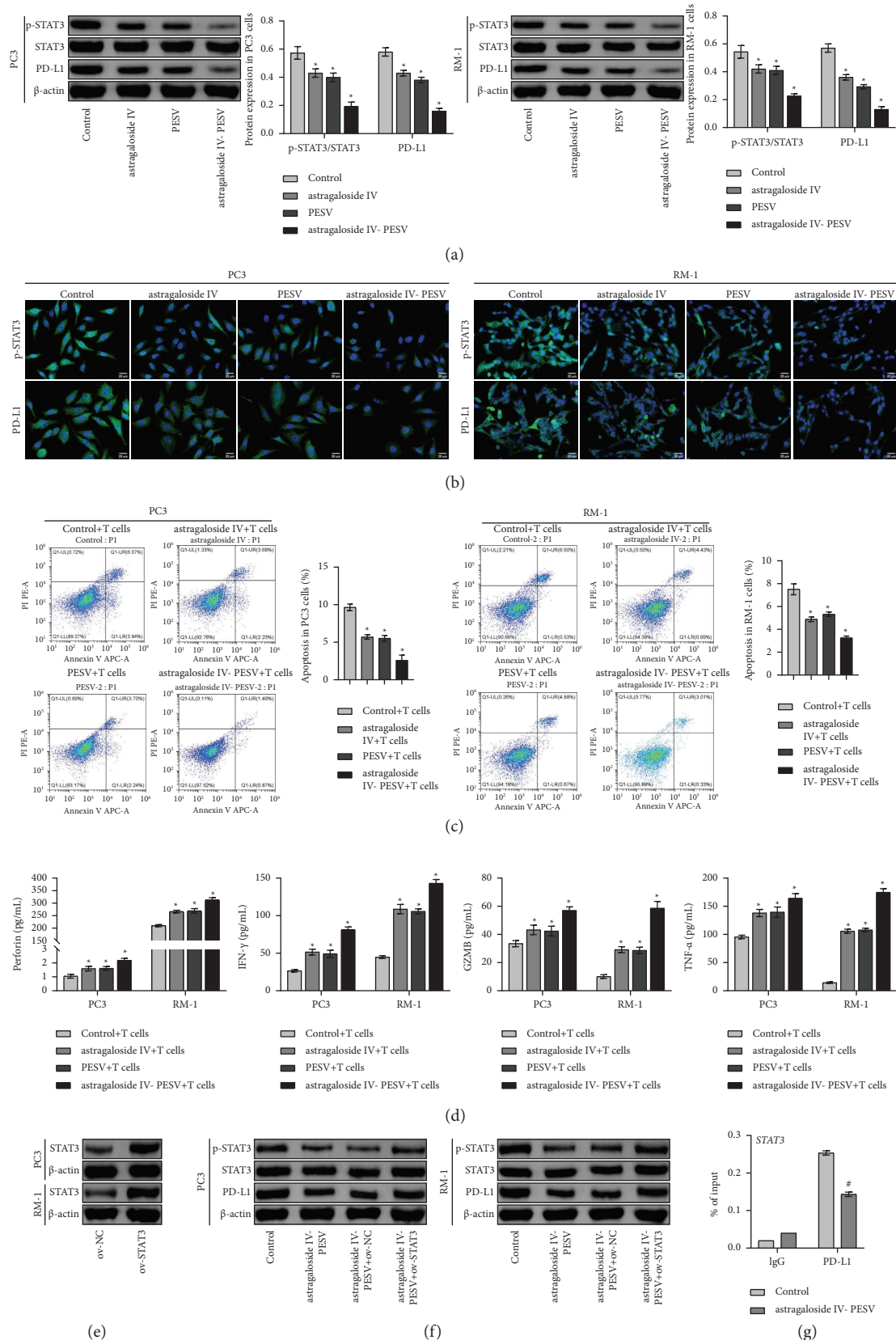
FIGURE 3: Astragaloside IV-PESV suppressed PD-L1 levels by inhibiting STAT3 signaling to regulate immunity. (a, b) The p-STAT3, STAT3, and PD-L1 expression levels in PC3 cells treated with astragaloside IV-PESV were determined by western blot or IF. $^*P < 0.05$ vs. Control. (c) Flow cytometry detection of T cell apoptosis. (d) ELISA detection of the expression levels of T cell supernatant IFN-γ, TNF-α, GZMB, and Perforin. $^*P < 0.05$ vs. Control + T cells. (e) STAT3 level. (f) p-STAT3, STAT3, and PD-L1 levels. (g) ChIP experiments demonstrated that astragaloside IV-PESV inhibited the binding of STAT3 to the PD-L1 promoter. $^\&P < 0.05$ vs. Control.
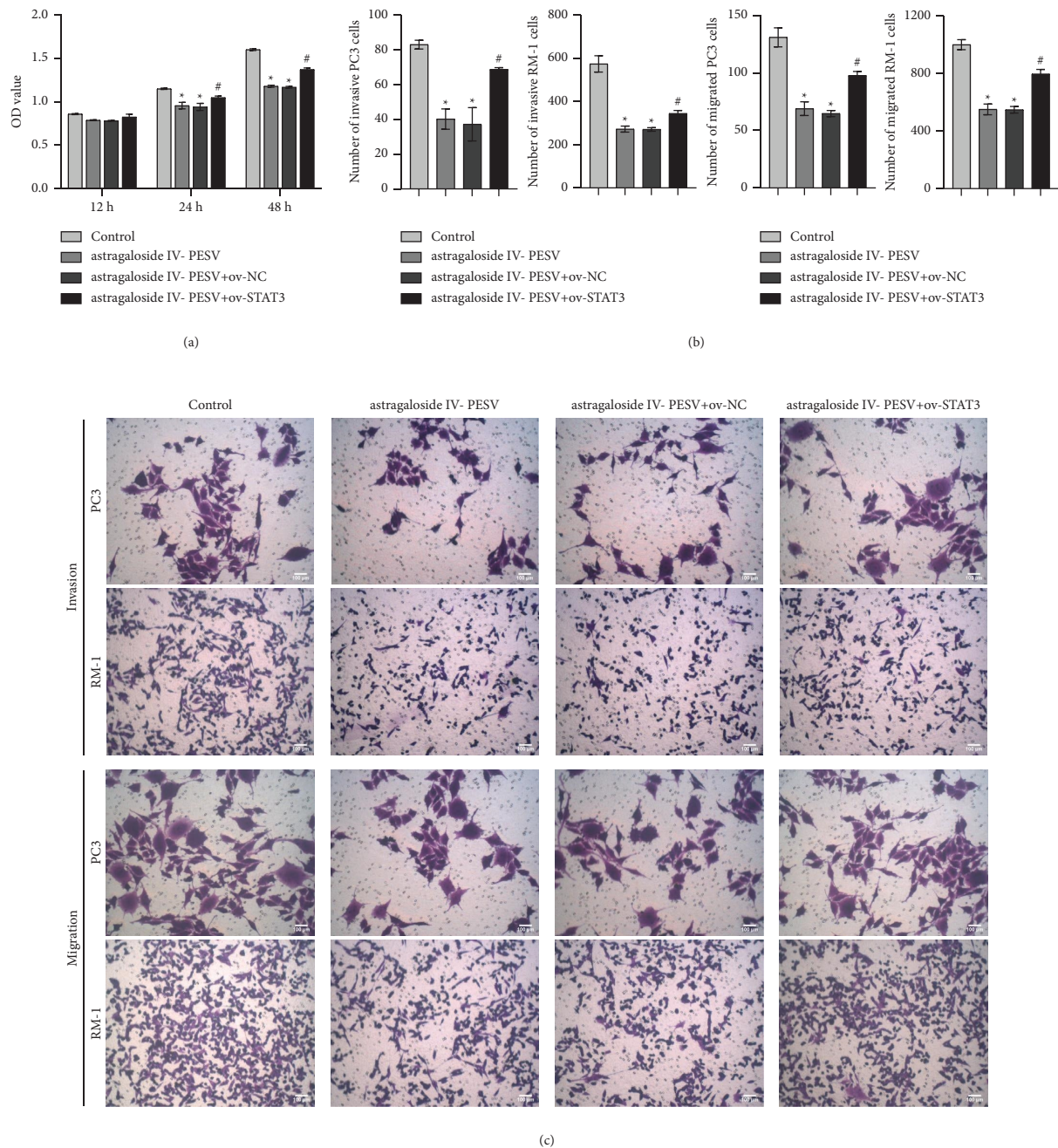
(a)

(b)

(c)

FIGURE 4: Overexpression of STAT3 reversed the inhibitory effects of astragaloside IV-PESV on PCa cell function. (a) CCK-8 assay of cell proliferation. (b, c) Transwell assays of cell migration and invasion. $^*P < 0.05$ vs. Control; $^{\#}P < 0.05$ vs. astragaloside IV-PESV + ov-NC.

results indicated that overexpression of STAT3 reversed the inhibitory effects of astragaloside IV-PESV on PCa cell proliferation, migration, and invasion.

3.5. Overexpression of STAT3 Reversed the Promoting Effect of Astragaloside IV-PESV on T Cell Activation.

Next, we examined the effect of overexpression of STAT3 on T cells. Compared with the Control + T cells group, the astragaloside IV-PESV + T cells group showed reduced T cell apoptosis and increased cell supernatant IFN-γ, TNF-α, GZMB, and Perforin expression levels. In contrast, after

overexpression of STAT3, T cell apoptosis increased and supernatant IFN-γ, TNF-α, GZMB, and Perforin levels decreased (Figures 5(a)–5(c)). These results suggested that overexpression of STAT3 reversed the promoting effect of astragaloside IV-PESV on T cell activation.

3.6. Overexpression of STAT3 Reversed Astragaloside IV-PESV Effects on Immune Escape In Vivo.

Finally, we further validated the effects of ov-STAT3 on immune escape *in vivo*. Compared with the ov-NC group, the tumor volume and weight were observably elevated in the ov-STAT3 group, and
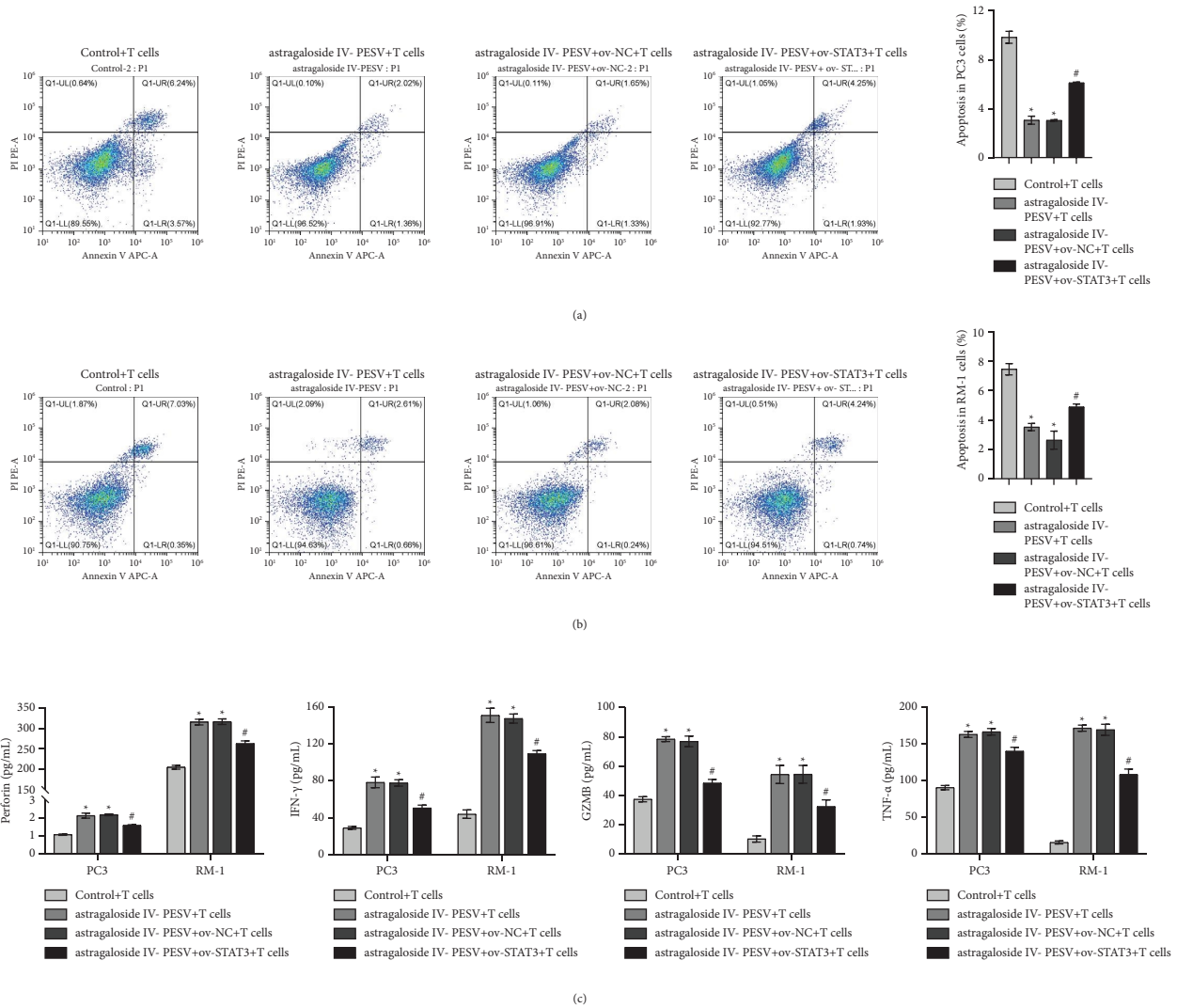
(a)

(b)

(c)

FIGURE 5: Overexpression of STAT3 reversed the promoting effect of astragaloside IV-PESV on T cell activation. (a, b) Flow cytometry detection for T cell apoptosis. (c) ELISA detection for T cell supernatant IFN-γ, TNF-α, GZMB, and Perforin levels. $^*P < 0.05$ vs. Control + T cells; $^{\#}P < 0.05$ vs. astragaloside IV-PESV + ov-NC + T cells.

Ki-67 expression was increased. After administration of astragaloside IV-PESV, the tumor volume and weight were significantly reduced, and Ki-67 expression was decreased (Figures 6(a)–6(c)). Compared with the ov-NC group, overexpression of STAT3 downregulated CD8 levels in tumor tissues. After administration of astragaloside IV-PESV, CD8 levels increased (Figure 6(d)). After overexpression of STAT3, CD3+ CD8+ T cell levels in cancer tissues and peripheral blood were significantly reduced. After administration of astragaloside IV-PESV again, CD3+ CD8+ T cell levels increased (Figure 6(e)). In addition, IFN-γ, TNF-α, GZMB, and Perforin levels in peripheral blood were reduced after overexpression of STAT3 (Figure 6(f)). STAT3, p-STAT3, and PD-L1 levels were higher in the ov-STAT3 group than in the ov-NC group (Figure 6(g)). The levels of these indicators were reversed after further administration of astragaloside IV-PESV. Collectively, overexpression of STAT3 reversed astragaloside IV-PESV effects on immune escape.

4. Discussion

PCa is traditionally considered an immune "cold" tumor with a low mutational burden, low PD-L1 expression, sparse T-cell infiltration, and an immunosuppressive tumor microenvironment [27]. In the research, we explored the role of astragaloside IV-PESV in regulating tumor immune microenvironment in PCa based on STAT3/PD-L1 signaling pathway, combined with *in vitro* and *in vivo* experiments, and elucidated its molecular mechanism. We showed that astragaloside IV-PESV repressed T cell immunosuppression by inhibiting PD-L1 expression in PCa via the STAT3 pathway. Our study provides a new strategy for immunotherapy in PCa.

Astragaloside IV, a natural saponin isolated from *Astragalus*, is a cycloalkane-type triterpene glycoside compound with antioxidant, anti-inflammatory, antiviral, antibacterial, and immunomodulatory effects [28]. Additionally, astragaloside IV also exerts antitumor effects,
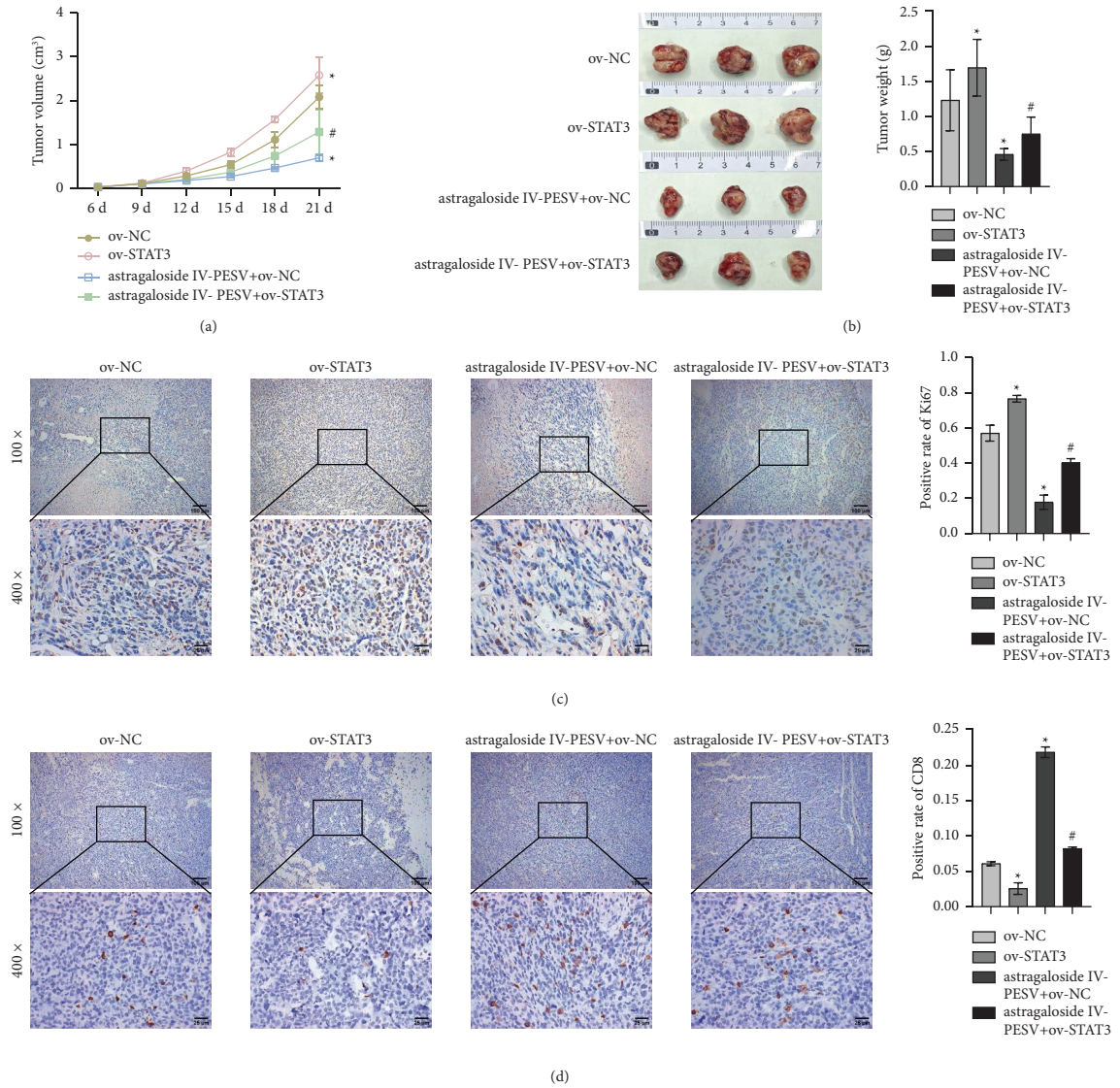
(a)
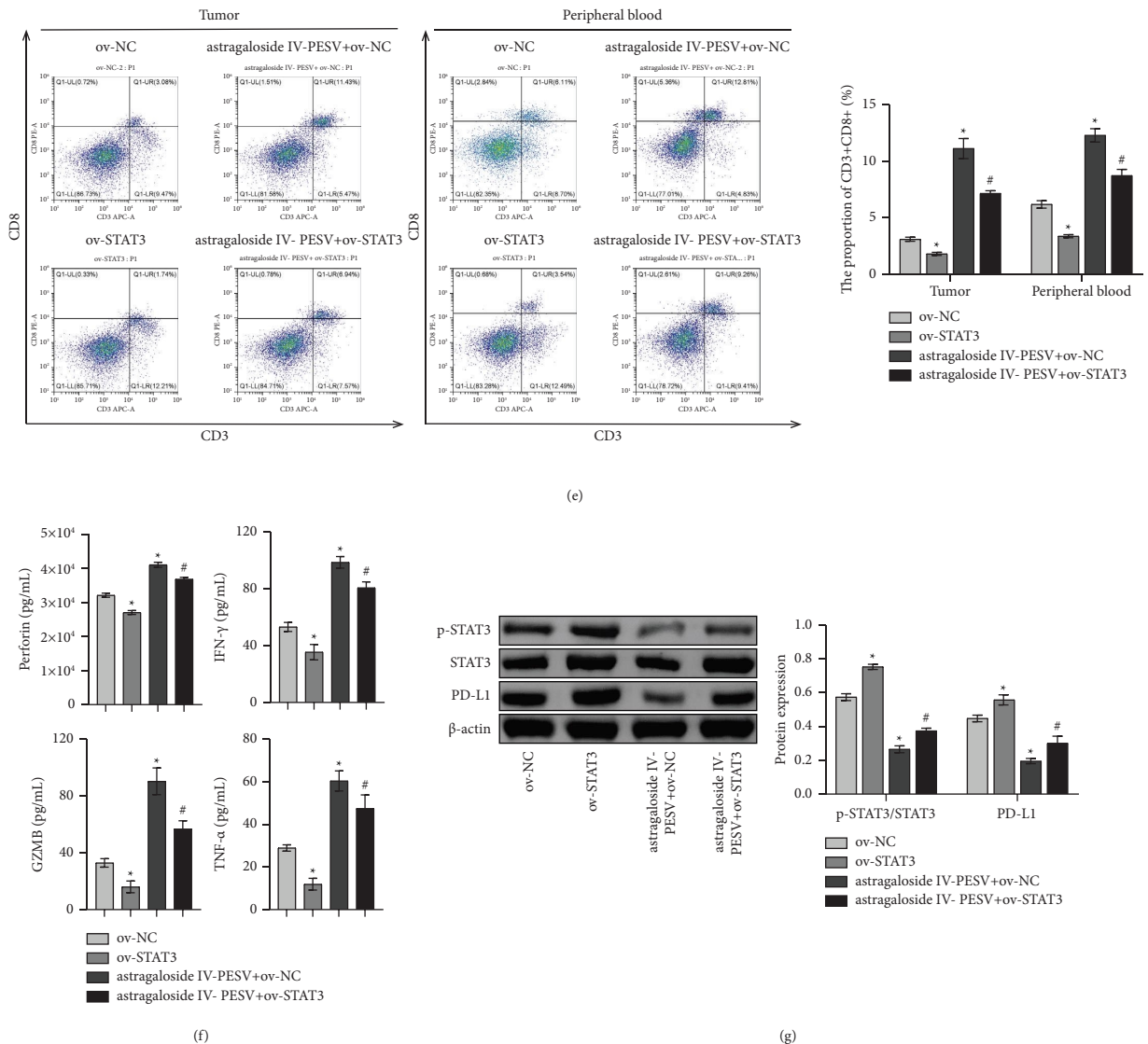
(b)

(c)

(d)

Figure 6: Continued.

(e)

(f)

(g)

FIGURE 6: Overexpression of STAT3 reversed the effect of astragaloside IV-PESV on immune escape *in vivo*. (a) Tumor volume. (b) The image of tumor tissues and the weight of tumor tissues. (c) IHC analysis for Ki-67 expression. (d) IHC analysis for CD8 expression. (e) Flow cytometry detection for CD3 +CD8+ T cell levels in tumor tissues and peripheral blood. (f) ELISA detection for IFN-γ, TNF-α, GZMB, and Perforin levels in peripheral blood. (g) p-STAT3, STAT3, and PD-L1 levels in tumor tissues. *$P < 0.05$ vs. ov-NC; #$P < 0.05$ vs. astragaloside IV-PESV + ov-NC.

including breast [29], liver [30], lung [31], and gastric [32] cancers. In PCa, astragaloside IV also plays an important role [20, 21]. Scorpion has an activating effect, and PESV could inhibit the proliferation of NSCLC cells [33], induce apoptosis in lung cancer cells [34], and inhibit the development of H22 liver cancer transplantation tumors in mice [35]. In addition, PESV could also induce apoptosis in PCa cells DU145 [22]. Our previous study found that combining astragaloside IV and PESV exerted the antitumor effects in PCa [20]. On this basis, we then explored the modulatory effect of astragaloside IV-PESV on the cancer immune microenvironment. In the present study, we first verified the binding of astragaloside IV and PESV to STAT3 and PD-L1

by molecular docking. We then explored the effect of astragaloside IV-PESV on tumor immunity and the STAT3/PD-L1 pathway.

PD-L1 is closely related to the immune escape process of tumor cells [36]. A blockade of PD-1/PD-L1 is usually considered to have a great deal of effect depending upon the expression of PD-L1, the availability of cytotoxic T lymphocytes, and the magnitude of tumor mutations [37]. Cancer cells evade immune detection by inactivating T cells via PD-1/PD-L1 interactions [38]. Anti-PD-1/PD-L1 therapy aims to restore the antitumor response of cytotoxic T cells by blocking the interaction between PD-L1 on cancer cells and PD-1 on cytotoxic T cells [39]. Therefore, exploring

the underlying mechanisms of PD-L1 regulation in cancer cells is one way to target the reduction of PD-L1 levels and thus make drug-resistant cancer cells respond to PD-1/PD-L1 antibody therapy. Zhang et al. reported that Chinese medicine CFF-1 inhibited the PD-1/PD-L1 checkpoint signaling pathway via EGFR/JAK1/STAT3 pathway and played an antitumor immune role in inhibiting tumor growth and metastasis in PCa [40]. Lee et al. revealed that ginseng saponin metabolite compound K could induce apoptosis in PCa cells by inhibiting the STAT3/PD-L1 signaling pathway [41]. This demonstrates the antitumor potential of TCM in PCa. Our study showed that *in vivo*, astragaloside IV-PESV repressed immunosuppression and STAT3/PD-L1 pathway. *In vitro*, astragaloside IV-PESV suppressed PD-L1 expression by inhibiting STAT3 signaling to modulate immunity. *In vivo* and *in vitro* experiments validated that the antitumor and immunomodulatory effects of astragaloside IV-PESV were associated with the STAT3/PD-L1 pathway. Thus, next, we further explored the role of overexpression of STAT3 in the anti-PCa of astragaloside IV-PESV.

STAT3 mediates various gene expressions that play key roles in many cellular and biological processes, including cell proliferation, angiogenesis, and inflammation [42]. STAT3 signaling pathway regulates immune factor expression, recruits immunosuppressive cells, and creates the immunosuppressive environment [43]. Xu et al. suggested that combined inhibition of JAK1, 2/PD-L1, and STAT3/PD-L1 pathway may heighten immune cytolytic activity of natural killer cells in response to hypoxia-induced denervation-resistant PCa cells [44]. Xu et al. revealed that inhibiting the IL-6-JAK/STAT3 pathway in denervation-resistant PCa cells enhanced natural killer cell-mediated cytotoxicity by altering PD-L1/NKG2D ligand levels [45]. We demonstrated that overexpression of STAT3 reversed the inhibitory effects of astragaloside IV-PESV on PCa cell function and promoted T cell activation *in vitro*. *In vivo* experiments further illuminated that overexpression of STAT3 reversed astragaloside IV-PESV effects on immune escape.

However, this study has some limitations. In this study, to explore the regulatory effect of astragaloside IV-PESV on the tumor immune microenvironment, we only studied T cells. The role of other immune cells such as macrophages, dendritic cells, natural killer (NK) cells, myeloid-derived suppressor cells (MDSC), and CD4 to CD8 ratio was not studied. In the future, to further investigate the regulatory effect of Astragaloside IV-PESV on the tumor immune microenvironment, we will explore the role of other immune cells such as macrophages, dendritic cells, NK cells, MDSC, and CD4 to CD8 ratio.

5. Conclusions

In this study, we initially assessed the relationship of astragaloside IV and PESV with STAT3 and PD-L1 using molecular docking. We explored the role of astragaloside IV-PESV in regulating the tumor immune microenvironment in PCa. Through *ex vivo* experiments, we found that astragaloside IV-PESV repressed T cell immunosuppression by inhibiting PD-L1 expression in PCa through the STAT3 pathway. Our findings suggest an antitumor mechanism of astragaloside IV-PESV in PCa and also provide novel targets and strategies for treating PCa.

Data Availability

The data used to support the findings of this study are included within the article and supplementary information file.

Conflicts of Interest

The authors declare that they have no conflicts of interest.

Acknowledgments

Supplementary Materials

Supplementary Figure S1: the expression of STAT3, p-STAT3, and PD-L1. (A) p-STAT3 and PD-L1 levels in PC3 cells treated with astragaloside IV-PESV were determined by IF. (B) STAT3 level. (C) p-STAT3, STAT3, and PD-L1 levels. $^*P < 0.05$ vs. Control; $^#P < 0.05$ vs. astragaloside IV-PESV + ov-NC. (*Supplementary Materials*)

References

[1] M. Sekhoacha, K. Riet, P. Motloung, L. Gumenku, A. Adegoke, and S. Mashele, "Prostate cancer review: genetics, diagnosis, treatment options, and alternative approaches," *Molecules*, vol. 27, no. 17, p. 5730, 2022.

[2] M. C. Haffner, W. Zwart, M. P. Roudier et al., "Genomic and phenotypic heterogeneity in prostate cancer," *Nature Reviews Urology*, vol. 18, no. 2, pp. 79–92, 2021.

[3] R. J. Rebello, C. Oing, K. E. Knudsen et al., "Prostate cancer," *Nature Reviews Disease Primers*, vol. 7, no. 1, p. 9, 2021.

[4] S. D. Lokeshwar, Z. Klaassen, and F. Saad, "Treatment and trials in non-metastatic castration-resistant prostate cancer," *Nature Reviews Urology*, vol. 18, no. 7, pp. 433–442, 2021.

[5] K. Kolijn, E. I. Verhoef, M. Smid et al., "Epithelial-mesenchymal transition in human prostate cancer demonstrates enhanced immune evasion marked by Ido1 expression," *Cancer Research*, vol. 78, no. 16, pp. 4671–4679, 2018.

[6] C. Antognelli, R. Cecchetti, F. Riuzzi, M. J. Peirce, and V. N. Talesa, "Glyoxalase 1 sustains the metastatic phenotype of prostate cancer cells via EMT control," *Journal of Cellular and Molecular Medicine*, vol. 22, no. 5, pp. 2865–2883, 2018.

[7] Q. H. Chen, B. Li, D. G. Liu, B. Zhang, X. Yang, and Y. L. Tu, "LncRNA KCNQ1OT1 sponges miR-15a to promote immune evasion and malignant progression of prostate cancer via up-

regulating PD-L1," *Cancer Cell International*, vol. 20, no. 1, p. 394, 2020.

[8] C. Antognelli, M. Mandarano, E. Prosperi, A. Sidoni, and V. N. Talesa, "Glyoxalase-1-Dependent methylglyoxal depletion sustains PD-L1 expression in metastatic prostate cancer cells: a novel mechanism in cancer immunosurveillance escape and a potential novel target to overcome PD-L1 blockade resistance," *Cancers*, vol. 13, no. 12, p. 2965, 2021.

[9] Y. Zhang, S. Zhu, Y. Du et al., "RelB upregulates PD-L1 and exacerbates prostate cancer immune evasion," *Journal of Experimental and Clinical Cancer Research*, vol. 41, no. 1, p. 66, 2022.

[10] H. B. Gupta, C. A. Clark, B. Yuan et al., "Tumor cell-intrinsic PD-L1 promotes tumor-initiating cell generation and functions in melanoma and ovarian cancer," *Signal Transduction and Targeted Therapy*, vol. 1, Article ID 16030, 2016.

[11] S. Xue, M. Hu, P. Li et al., "Relationship between expression of PD-L1 and tumor angiogenesis, proliferation, and invasion in glioma," *Oncotarget*, vol. 8, no. 30, pp. 49702–49712, 2017.

[12] C. Y. Ock, S. Kim, B. Keam et al., "PD-L1 expression is associated with epithelial-mesenchymal transition in head and neck squamous cell carcinoma," *Oncotarget*, vol. 7, no. 13, pp. 15901–15914, 2016.

[13] C. Sun, R. Mezzadra, and T. N. Schumacher, "Regulation and function of the PD-L1 checkpoint," *Immunity*, vol. 48, no. 3, pp. 434–452, 2018.

[14] M. Lopez de Rodas, V. Nagineni, A. Ravi et al., "Role of tumor infiltrating lymphocytes and spatial immune heterogeneity in sensitivity to PD-1 axis blockers in non-small cell lung cancer," *Journal of Immunother Cancer*, vol. 10, no. 6, Article ID e004440, 2022.

[15] D. D. Shen, J. R. Pang, Y. P. Bi et al., "LSD1 deletion decreases exosomal PD-L1 and restores T-cell response in gastric cancer," *Molecular Cancer*, vol. 21, no. 1, p. 75, 2022.

[16] L. G. Lu, Z. L. Zhou, X. Y. Wang et al., "PD-L1 blockade liberates intrinsic antitumourigenic properties of glycolytic macrophages in hepatocellular carcinoma," *Gut*, vol. 71, no. 12, pp. 2551–2560, 2022.

[17] D. Y. Kang, N. Sp, J. M. Lee, and K. J. Jang, "Antitumor effects of ursolic acid through mediating the inhibition of STAT3/PD-L1 signaling in non-small cell lung cancer cells," *Biomedicines*, vol. 9, no. 3, p. 297, 2021.

[18] S. Q. Sun, Y. X. Zhao, S. Y. Li, J. W. Qiang, and Y. Z. Ji, "Antitumor effects of astaxanthin by inhibition of the expression of STAT3 in prostate cancer," *Marine Drugs*, vol. 18, no. 8, p. 415, 2020.

[19] X. Zhou, L. Zou, H. Liao et al., "Abrogation of HnRNP L enhances anti-PD-1 therapy efficacy via diminishing PD-L1 and promoting CD8(+) T cell-mediated ferroptosis in castration-resistant prostate cancer," *Acta Pharmaceutica Sinica B*, vol. 12, no. 2, pp. 692–707, 2022.

[20] X. You, Y. Wu, Q. Li, W. Sheng, Q. Zhou, and W. Fu, "Astragalus-scorpion drug pair inhibits the development of prostate cancer by regulating GDPD4-2/PI3K/AKT/mTOR pathway and autophagy," *Frontiers in Pharmacology*, vol. 13, Article ID 895696, 2022.

[21] Y. He, Q. Zhang, H. Chen et al., "Astragaloside IV enhanced carboplatin sensitivity in prostate cancer by suppressing AKT/NF-κB signaling pathway," *Biochemistry and Cell Biology*, vol. 99, no. 2, pp. 214–222, 2021.

[22] Y. Y. Zhang, L. C. Wu, Z. P. Wang et al., "Anti-proliferation effect of polypeptide extracted from scorpion venom on human prostate cancer cells in vitro," *Journal of Clinical Medicine Research*, vol. 1, no. 1, pp. 24–31, 2009.

[23] Z. W. Luo, K. Xia, Y. W. Liu et al., "Extracellular vesicles from akkermansia muciniphila elicit antitumor immunity against prostate cancer via modulation of CD8(+) T cells and macrophages," *International Journal of Nanomedicine*, vol. 16, pp. 2949–2963, 2021.

[24] X. Xu, L. Niu, Y. Liu et al., "Study on the mechanism of Gegen Qinlian Decoction for treating type II diabetes mellitus by integrating network pharmacology and pharmacological evaluation," *Journal of Ethnopharmacology*, vol. 262, Article ID 113129, 2020.

[25] J. S. Wu, S. R. Sheng, X. H. Liang, and Y. L. Tang, "The role of tumor microenvironment in collective tumor cell invasion," *Future Oncology*, vol. 13, no. 11, pp. 991–1002, 2017.

[26] K. Huang, C. Fang, K. Yi et al., "The role of PTRF/Cavin1 as a biomarker in both glioma and serum exosomes," *Theranostics*, vol. 8, no. 6, pp. 1540–1557, 2018.

[27] I. Wang, L. Song, B. Y. Wang, A. Rezazadeh Kalebasty, E. Uchio, and X. Zi, "Prostate cancer immunotherapy: a review of recent advancements with novel treatment methods and efficacy," *American Journal of Clinical and Experimental Urology*, vol. 10, no. 4, pp. 210–233, 2022.

[28] J. Zhang, C. Wu, L. Gao, G. Du, and X. Qin, "Astragaloside IV derived from Astragalus membranaceus: a research review on the pharmacological effects," *Advances in Pharmacology*, vol. 87, pp. 89–112, 2020.

[29] S. Hu, W. Zheng, and L. Jin, "Astragaloside IV inhibits cell proliferation and metastasis of breast cancer via promoting the long noncoding RNA TRHDE-AS1," *Journal of Natural Medicines*, vol. 75, no. 1, pp. 156–166, 2021.

[30] C. Zhang, L. Li, S. Hou et al., "Astragaloside IV inhibits hepatocellular carcinoma by continually suppressing the development of fibrosis and regulating pSmad3C/3L and Nrf2/HO-1 pathways," *Journal of Ethnopharmacology*, vol. 279, Article ID 114350, 2021.

[31] F. Xu, W. Q. Cui, Y. Wei et al., "Astragaloside IV inhibits lung cancer progression and metastasis by modulating macrophage polarization through AMPK signaling," *Journal of Experimental and Clinical Cancer Research*, vol. 37, no. 1, p. 207, 2018.

[32] F. Li, K. Cao, M. Wang, Y. Liu, and Y. Zhang, "Astragaloside IV exhibits anti-tumor function in gastric cancer via targeting circRNA dihydrolipoamide S-succinyltransferase (circDLST)/miR-489-3p/eukaryotic translation initiation factor 4A1(EIF4A1) pathway," *Bioengineered*, vol. 13, no. 4, pp. 10112–10123, 2022.

[33] H. Zhang, H. Zhang, J. Zhu, H. Liu, and Q. Zhou, "PESV represses non-small cell lung cancer cell malignancy through circ_0016760 under hypoxia," *Cancer Cell International*, vol. 21, no. 1, p. 628, 2021.

[34] Y. N. Ning, W. D. Zhang, and L. C. Wu, "[Study on the mechanism of polypeptide extract from scorpion venom to promote the restraint of cyclophosphamide on Lewis lung cancer]," *Zhongguo Zhong Xi Yi Jie He Za Zhi*, vol. 32, no. 4, pp. 537–542, 2012.

[35] Q. Q. Zhao, W. D. Zhang, L. C. Wu et al., "[Mechanism of polypeptide extract from scorpion venom combined rapamycin in enhancing autophagy of H22 hepatoma cells: an experimental study]," *Zhongguo Zhong Xi Yi Jie He Za Zhi*, vol. 35, no. 7, pp. 866–870, 2015.

[36] R. Zhang, Z. Meng, X. Wu, M. Zhang, Z. Piao, and T. Jin, "PD-L1/p-STAT3 promotes the progression of NSCLC cells by

regulating TAM polarization," *Journal of Cellular and Molecular Medicine*, vol. 26, no. 23, pp. 5872–5886, 2022.

[37] L. Ai, A. Xu, and J. Xu, "Roles of PD-1/PD-L1 pathway: signaling, cancer, and beyond," *Advances in Experimental Medicine and Biology*, vol. 1248, pp. 33–59, 2020.

[38] Q. Li, Z. W. Zhou, J. Lu et al., "PD-L1(P146R) is prognostic and a negative predictor of response to immunotherapy in gastric cancer," *Molecular Therapy*, vol. 30, no. 2, pp. 621–631, 2022.

[39] J. H. Li, L. J. Huang, H. L. Zhou et al., "Engineered nanomedicines block the PD-1/PD-L1 axis for potentiated cancer immunotherapy," *Acta Pharmacologica Sinica*, vol. 43, no. 11, pp. 2749–2758, 2022.

[40] Y. Zhang, Y. Wei, S. Jiang et al., "Traditional Chinese medicine CFF-1 exerts a potent anti-tumor immunity to hinder tumor growth and metastasis in prostate cancer through EGFR/JAK1/STAT3 pathway to inhibit PD-1/PD-L1 checkpoint signaling," *Phytomedicine*, vol. 99, Article ID 153939, 2022.

[41] J. H. Lee, D. Y. Lee, H. J. Lee et al., "Inhibition of STAT3/PD-L1 and activation of miR193a-5p are critically involved in apoptotic effect of compound K in prostate cancer cells," *Cells*, vol. 10, no. 8, p. 2151, 2021.

[42] F. Zhu, K. B. Wang, and L. Rui, "STAT3 activation and oncogenesis in lymphoma," *Cancers*, vol. 12, no. 1, p. 19, 2019.

[43] L. Zhang, K. Kuca, L. You et al., "Signal transducer and activator of transcription 3 signaling in tumor immune evasion," *Pharmacology & Therapeutics*, vol. 230, Article ID 107969, 2022.

[44] L. J. Xu, Q. Ma, J. Zhu et al., "Combined inhibition of JAK1,2/Stat3-PD-L1 signaling pathway suppresses the immune escape of castration-resistant prostate cancer to NK cells in hypoxia," *Molecular Medicine Reports*, vol. 17, no. 6, pp. 8111–8120, 2018.

[45] L. Xu, X. Chen, M. Shen et al., "Inhibition of IL-6-JAK/Stat3 signaling in castration-resistant prostate cancer cells enhances the NK cell-mediated cytotoxicity via alteration of PD-L1/NKG2D ligand levels," *Molecular Oncology*, vol. 12, no. 3, pp. 269–286, 2018.